

Robert STRAKOWSKI, Bogusław WIĘCEK
 LODZ UNIVERSITY OF TECHNOLOGY, INSTITUTE OF ELECTRONICS
 211/215 Wólczańska St., 90-924 Łódź, Poland

A simplified model of parasitic radiation in IR bolometer camera

Abstract

This article presents the impact of thermal radiation of the internal elements of the camera on temperature and its distribution on the bolometers of the Focal Plane Array. In order to estimate the effect of this component, a simplified radiation heat transfer model was created for the detector, the object and the camera housing. The model is based on the known term of radiation configuration factors. It was also suggested to use a radiation screen to isolate the detector from the influence of the camera housing. Finally, results of numerical simulations for different camera work conditions are presented.

Keywords: radiation model, configuration factor, uncooled camera, residual non uniformity, heat exchange.

1. Introduction

The bolometric camera operates on the principle of radiation heat transfer between the detector and the object observed through the optics. When the detector temperature is lower than the object temperature, the object's radiation heats the sensor and its temperature rises. In the opposite case, the detector is cooled by the flow of radiation energy from the detector to the object. Unfortunately, not all energy transferred from/to the object is transmitted through the optical system of the camera. That is due to the transmissivity of the lens material and optics geometry. Assuming 100% transmissivity and F/1 optics, only one fourth of the object energy falls on the Focal Plane Array (FPA) [1].

Moreover, not only the radiation from the observed scene affects the detectors of the FPA. All internal parts of the camera radiate considerable amount of energy in the Long Wavelength InfraRed spectrum, LWIR, $\lambda \in (7,14) \mu\text{m}$, the typical uncooled camera works in. What is worse, as they are located behind the optical system, they affect significantly the temperature change of the FPA detectors. This radiation is undesirable, it disrupts the temperature measurement of the observed object [2]. Due to above, it could be specified as parasitic radiation. This is the direct cause of a large part of the thermal drift effect of the detectors. Most part of this effect is corrected with the use of mechanical shutter and One Point Non-Uniformity Correction (*1pNUC*). The shutter is located between the FPA and the optics, and there are parts of the camera, thermal radiation is not corrected [3].

The purpose of this paper is to estimate the influence of the different radiation power levels of the structural components of the camera, which affect the total radiation energy coming to or emitted from a single detector of FPA and the observed object. In the developed model, the detector substrate is not considered. Thus, heat conduction through the heat sink on which the detector array is placed is neglected. Moreover, the detector temperature was assumed to be stabilized at constant value of 25°C.

Two cases of internal camera structure were investigated: with and without the radiation screen stabilized to the temperature of the detector. It can be shown that the radiation of the side (S_2) and front (S_3) elements of the camera housing result in both thermal drift and Residual Non-Uniformity (RNU) [4].

2. Radiation configuration factors

In the theory of heat exchange and radiation heat transfer there is a known term of radiation configuration factors [1, 5]. The configuration factor F_{1-2} indicates what part of the radiation energy emitted to half-space from body 1 reaches body 2. For objects of infinitely small dimensions, the coefficient is marked with the symbol F_{d1-d2} . If the heat exchange occurs between the

element dS_1 and the surface S_2 of finite size, the configuration factor F_{d1-2} is determined. The last case is considered in the paper.

The single detector of FPA is considered to be an infinitely small object with a surface of dS_D that will exchange energy with such elements as: the lens (S_1), the front element of the camera housing (S_2), the side element of the camera housing (S_3) and finally in the second case the radiation screen (S_4). The position of these elements in the model is presented in Fig. 1.

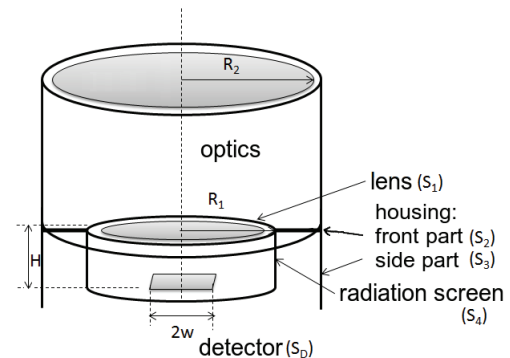


Fig. 1. The scheme of the camera structural components in its front section used for designed model

Figure 2 presents two cases of camera setup that were investigated in the research. First (Fig.2a) is without and second is with (Fig.2b) the radiation screen that isolates the detector from the influence of the camera housing. All camera structural components have different values of configuration factors with the detector. This results from their different shape, size and position according to bolometer detector. What is more, the FPA contains many detectors that are located near the focusing plane but at different distances from the optical axis of the camera and the lens. Therefore, the configuration factor between each surface (i.e. lens S_1) and every FPA detector also varies. In order to calculate the influence of camera structural components on temperature change of all detectors of FPA, each of configuration factors had to be determined.

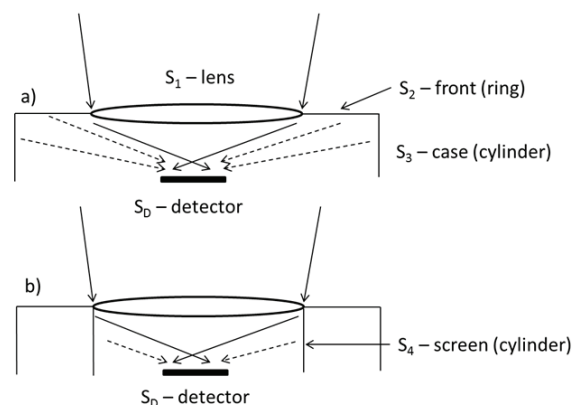


Fig. 2. The simple scheme of two camera setups that were investigated with marked radiation that falls on the detector: a) without radiation screen, b) with radiation screen

2.1. The configuration factor of the radiation from the observed object that falls on the single detector

The largest part of the radiation energy falling on the detector comes from the investigated object. This radiation passes through the optics. In thermal cameras optical system usually consists of 2 lenses, as in Fig.1. More lenses would not provide a high transmission value, which would result in lower camera sensitivity. For the same reason, lenses with a low F number value are not used in thermal imaging cameras.

The object's radiation passing through the optics falls on a single detector. Applying the reciprocity principle [5], it can be shown that:

$$F_{dD-1}S_D = F_{O-D}S_O \quad (1)$$

where: F_{dD-1} is detector-lens configuration factor, S_D is the surface area of the single detector, F_{O-D} is object-single detector configuration factor and S_O is surface area of the object.

Due to above the configuration factor, F_{O-D} takes form

$$F_{O-D} = F_{dD-1} \frac{S_D}{S_O} \quad (2)$$

To compute the power that falls on the single detector and is radiated from the object, the value of detector-lens (F_{dD-1}) configuration factor should be calculated. The value could be estimated analysing the geometric dependencies between these two elements, which are shown in Fig.3.

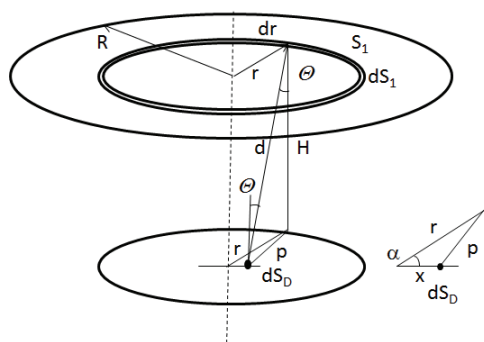


Fig. 3. Geometrical relations between a single detector of FPA and the second lens S1 of the camera optics system

Generally, configuration factors can be determined numerically by double integration [1, 5]. However, for the given detector-lens factor F_{dD-1} there is an analytical form given by Eq. 3 [6].

$$F_{dD-1} = \frac{1}{2} \left[1 - \frac{Z-2W^2}{\sqrt{Z^2-4W^2}} \right] \quad (3)$$

where: $Z = 1 + R^2/x^2 + H^2/x^2$, $W = R/x$.

2.2. The configuration factor of the radiation from the front element of the camera housing that falls on the single detector

The front element (S_2) of the camera housing camera is a ring (Fig.1). To determine value of its configuration factor a method of adding configuration factors of multiple surfaces were used [5]. The ring is the difference between two disk surfaces with a radius of R_2 and R_1 , what is shown in Fig.4.

In this case the configuration factor of the S_2 surface can be calculated as:

$$F_{dD-2} = F_{dD-12} - F_{dD-1} \quad (4)$$

where: symbol 1 presents a lens, symbol 12 presents the surface of the lens and the front element of the camera housing (S_1 & S_2). Surfaces 1 and 2 are disks with radiuses R_1 and R_2 respectively. In order to calculate F_{dD-2} with Eq.4, its two components should be calculated using Eq.3.

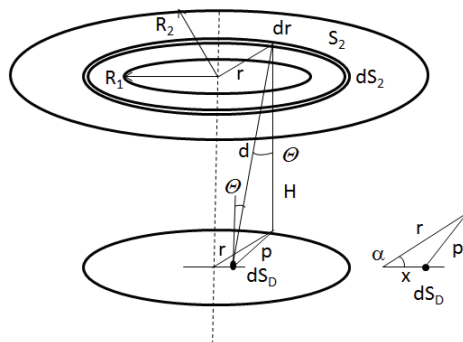


Fig. 4. Geometrical relations between a single detector of FPA and the front element of the camera housing which is a ring

2.3. The configuration factor of the radiation from the side element of the camera housing that falls on the single detector

It has been assumed that the side element of the camera housing (S_3) and the radiation screen (S_4) are cylindrical surfaces with the radiuses R_1 and R_2 respectively as shown in Fig.1. The inner surface of the cylinder could be described with the radius of the base R and the height H , as presented in Fig.5. Such a scheme applies to both the side part of camera housing and the radiation screen. The only difference is the value of radius. Analysing the presented geometrical relations, it was possible to determine the value of last two configuration factors that occur in the presented considerations (F_{dD-3} and F_{dD-4}). This factor represents the relation of heat transfer between a single detector and the inner surface of a cylinder.

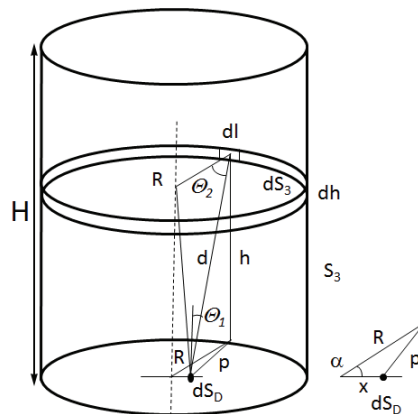


Fig. 5. Geometrical relations between a single detector of FPA and the side element of the camera housing (or radiation screen)

In the case of cylindrical surface S_3 and S_4 , its configuration factor takes form of Eq.5, according to the definition [5].

$$F_{dD-c} = \int_0^H \int_0^{2\pi R} \frac{\cos(\theta_1) \cos(\theta_2)}{\pi d^2} dh dl \quad (5)$$

Using relations presented in Fig.5 the final form of the configuration factor F_{dD-c} could be designated:

$$F_{dD-c} = \frac{R}{\pi} \int_0^H \int_0^{2\pi} \frac{h[R-2x \cos(\alpha)]}{[h^2+R^2+x^2-2Rx \cos(\alpha)]^2} dh d\alpha \quad (6)$$

3. Simplified radiation model

Knowledge of the configuration factors allows determining the value of the power delivered to or emitted by the single detector. Based on it, the change of the bolometer temperature could be calculated. This can be done applying the reciprocal principle for radiation heat transfer [5], which yields eq. (7). Consequently, the power of radiation, which falls on the detector from any considered surface $i = 1, 2, 3, 4$, could be expressed using eq. (8).

$$F_{dD-i} S_D = F_{i-dD} S_i \quad (7)$$

where: F_{dD-i} is the configuration factor of the detector for i surface of the camera interior and S_i is the area of this surface.

$$P_{i-dD} = \sigma F_{dD-i} S_D (T_i^4 - T_D^4) \quad (8)$$

where: $\sigma = 5,67 \cdot 10^{-8} \text{ W}/(\text{m}^2 \cdot \text{K}^4)$ is Stefan-Boltzmann constant, F_{dD-i} is a configuration factor for detector-surface number $i = 1, 2, 3, 4$, T_D is the value of the detector temperature ($T_D = 298,15 \text{ K}$), S_D is the surface area of single detector. In eq. (8) we have used the model of the black body radiation, while an IR camera is narrow-band device, and in consequence the energy affecting the detector is much lower. For LWIR range at temperature about 300 K, it is approximately $\frac{1}{4}$ of the total radiation energy [1]. This problem will be considered in the next stage of the research.

What is most significant, it was assumed that it is possible to stabilize the radiation screen temperature to the value close temperature of the detector. In this case, difference of two temperatures in Eq.8 is close to zero. In result, there is negligible radiation heat exchange between the screen and the detector. In effect, the FPA is isolated from the parasitic radiation of structural components of camera housing.

The change of single detector temperature value caused by the radiation heat exchange could be approximated by Eq.8. After simplification that the detector is ideally thermally insulated and the total radiated power changes only its temperature, the value of it could be estimated with eq. (9).

$$\Delta T_D = \frac{P t_{int}}{C_{th} V_D} \quad (9)$$

where: t_{int} is time of integration of bolometric camera detector, $V_D = S_D \cdot t_s$ is volume of single matrix detector, t_s is the detector thickness, $C_{th} = \rho c_w$ is heat capacity, ρ is density of matrix material, c_w is specific heat of the matrix material and P total radiation power reaching the detector.

For a camera without radiation screen, the radiated power is equal to

$$P = P_{1-dD} + P_{2-dD} + P_{3-dD}, \quad (10)$$

while for a camera with radiation screen

$$P = P_{1-dD} + P_{4-dD}. \quad (11)$$

The reader should note that the power P can be both positive and negative, which means the rise or fall in the detector's temperature value.

4. Simulation results

Simulations were made for the detector array of 384×288 pixels and the surface area of the single detector of $25 \times 25 \mu\text{m}$. It was

assumed that the detector thickness was $t_s = 100 \text{ nm}$ and the integration time $t_{int} = 100 \mu\text{s}$. The detector thermal parameters were: $\rho = 2300 \text{ kg}/\text{m}^3$ and $c_w = 712 \text{ J}/(\text{kg} \cdot \text{K})$. In addition, the following values of the detector and bolometric camera parameters were used: $R_1 = 0.04 \text{ m}$, $R_2 = 0.02 \text{ m}$, $H = 0.02 \text{ m}$ (see Fig.1).

In the model, the radiation of the FPA housing is omitted. It has been assumed that the effect of this radiation is corrected by a mechanical shutter during the $IpNUC$ procedure. The heat exchange by convection to the medium inside the detector housing and conduction to the substrate had also been omitted. In other words, the ideal thermal insulation of the FPA from the environment and substrate was assumed.

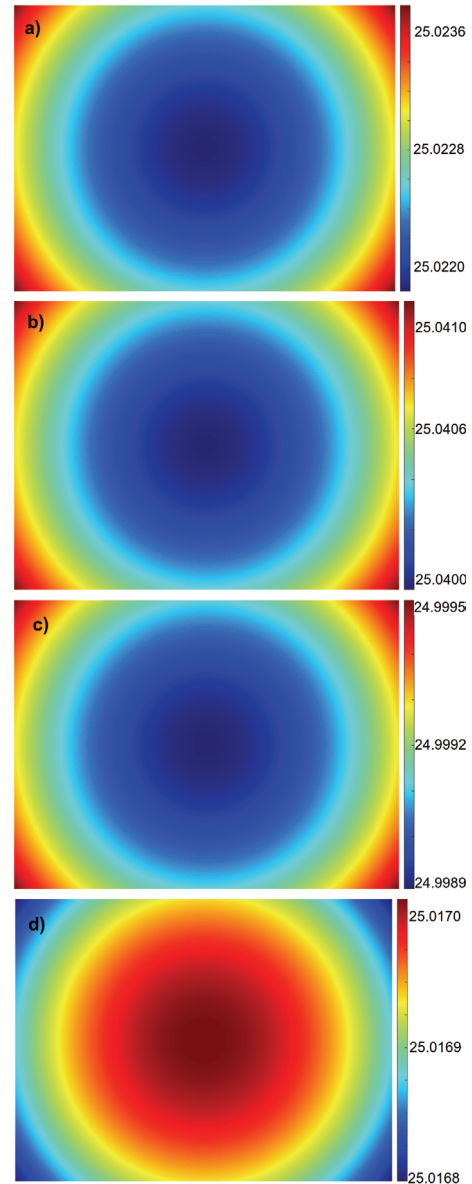


Fig. 6. Visualization of temperature distribution on the surface of the FPA for different temperature values of the observed object and with or without the use of radiation screen
a) $T_D = 25^\circ\text{C}$, $T_O = 20^\circ\text{C}$, $T_{\text{housing}} = 35^\circ\text{C}$, without radiation screen
b) $T_D = 25^\circ\text{C}$, $T_O = 30^\circ\text{C}$, $T_{\text{housing}} = 35^\circ\text{C}$, without radiation screen
c) $T_D = 25^\circ\text{C}$, $T_O = 20^\circ\text{C}$, $T_{\text{screen}} = 25^\circ\text{C}$, with radiation screen
d) $T_D = 25^\circ\text{C}$, $T_O = 30^\circ\text{C}$, $T_{\text{screen}} = 25^\circ\text{C}$, with radiation screen

The simulations were carried out for 2 cases: with and without the radiation screen. Furthermore, different temperature values of the object $T_O = T_1$ were investigated. The results are presented in Fig.6 as distributions of detectors' temperature across whole FPA, mapped using false colour scale.

The quantitative results of the simulations are presented in Tab.1. Four parameters of the matrix temperature distribution

were determined: mean, maximum, minimum and spread. It can be seen that the parasitic radiation emitted by the camera housing significantly influences the average temperature value of the surface of the matrix and its non-uniformity. As a result, after the calibration of the camera, the first effect will be the error of measuring the absolute temperature value of the observed object. The use of the radiation screen decreases the mean temperature offset of FPA for the observed object of same temperature. Secondly, it produces the relative measurement error of the temperature value from the pixels located at different position on the image (which corresponds to the position of detectors on the matrix). The use of a radiation screen has reduced the spread of FPA temperature values from 3 to 10 times.

Tab. 1. The values of the statistical parameters of temperature distribution on the surface of the FPA for the simulations shown in Fig. 6

Fig.	simulation parameters				FPA temperature parameters			
	T_D	T_O	T_{housing}	T_{screen}	mean	max	min	max-min
					°C			°C·10 ⁻⁴
6a	25	20	35	–	25.0225	25.0238	25.0218	19.47
6b	25	30	35	–	25.0403	25.0411	25.0399	11.42
6c	25	20	–	25	24.9990	24.9995	24.9989	6.33
6d	25	30	–	25	25.0169	25.0170	25.0168	1.72

5. Conclusions

The simulations allowed formulating conclusions that could be used during the design of thermal imaging cameras.

1. The radiation power of the bolometric camera housing, which causes the temperature to rise or fall, is comparable to the radiation output from the object. This means that the radiation of the camera housing components in front of the detector must not be ignored and the camera signal correction should be made to reduce the effect of this radiation.
2. Radiation of structural components affects both thermal drift and residual non-uniformity of the detector's signal.
3. The effect of the detector position on the FPA can cause both rise and fall of the bolometer temperature. As a consequence, the corners of the matrix can be both warmer and cooler relative to its center. What is more, the temperature distribution depends on the relation between the object temperature, the detector, and the housing components.
4. The use of the radiation screen effectively isolates the detector from the housing and reduces its impact on both drift and residual non-uniformity of the detector's signal. The use of the

screen requires thermal coupling with the detector so that the detector and screen temperature are equal.

6. References

- [1] Więcek B., Mey G. D.: Termowizja w podczerwieni, podstawy i zastosowania. Wydawnictwo PAK, 2011.
- [2] Mey G. D., Więcek B., Kałuża M., Olbrycht R., Strąkowski R., Strąkowska M.: Importance of radiative heat transfer for infrared thermography measurements, PAK, 57(10);1112-1115.
- [3] Tempelhahn A., Budzier H., Krause V., Gerlach G.: Modelling transient thermal behaviour of shutter-less microbolometer-based thermal cameras. Electro-Optical and Infrared Systems: Technology and Applications XI, volume 9249, 2014.
- [4] Fraenkel A., Mizrahi U., Bykov L., Adin A., Malkinson E., Zabar Y., Seter D., Gebil Y., Kopolovich Z.: Advanced features of SCD's uncooled detectors. Opto-Electronics Review, 14(1):46–53, March 2006.
- [5] Siegel R., Howell J. R.: Thermal Radiation Heat Transfer. McGraw-Hill, New York, 5th edition, 1971.
- [6] Howell J. R.: The catalogue of radiation heat transfer configuration factors, 3rd edition. University of Texas at Austin. 05.2017, <http://www.thermalradiation.net/indexCat.html>

Received: 15.11.2016

Paper reviewed

Accepted: 02.02.2017

Robert STRĄKOWSKI, MSc

Robert Strąkowski graduated from the Faculty of Electrical, Electronics, Computer and Control Engineering Lodz University of Technology. In The Department of Electronic Systems and Thermography he conducts research on the new method of signal correction from uncooled bolometers detectors. His research interests also include thermographic imaging and artificial neural networks.

e-mail: robert.strakowski@p.lodz.pl



Prof. Bogusław WIĘCEK

Bogusław Więcek is the head of Electronic Circuit and Thermography Division in Institute of Electronics where he has worked for more than 35 years. His scientific interests are: industrial and biomedical applications of IR thermography, heat transfer modelling and advanced IR analog and digital system developments. He is responsible for organizing the largest conference on thermography in Central and Eastern Europe every 2 years – Thermography and Thermometry Conference TTP.

e-mail: boguslaw.wiecek@p.lodz.pl

